CHARACTERIZATION OF FEEDSTOCK IN THE POWDER BED FUSION PROCESS: SOURCES OF VARIATION IN PARTICLE SIZE DISTRIBUTION AND THE FACTORS THAT INFLUENCE THEM

J. Whiting, J. Fox

Engineering Laboratory
National Institute of Standards and Technology, Gaithersburg, MD 20899

Abstract

Substantial efforts have been placed on characterizing and modeling additive manufacturing processes. The wide scope of work already done has focused on the effects of process parameters such as laser power, hatch spacing, scan speed and strategy, and layer thickness on the final part's properties. However, the characteristics of the actual powder should also be considered. The particles' size, morphology, roughness, and chemical composition will affect the final part properties including surface texture, density, tensile strength, and hardness. This paper will share some of the measurement methods used at the National Institute of Standards and Technology (NIST) to better understand metal powder for additive manufacturing. These include the striation/separation in transportation and handling, sampling procedures, and the actual spreading of powder in the laser powder bed fusion process. Results are presented that illustrate variations in the particle size distribution as a function of location on the build platform, substrate/part surface condition, and vertical position.

Keywords: Powder bed fusion; particle size distribution; powder spreading

1 Introduction

The powder bed fusion (PBF) process allows complex geometries to be additively manufactured (AM) in various metals and alloys. The process consists of a focused laser ($\approx 100\ \mu m$ spot size) that melts specific regions of metal powder. Between laser scans, the build area is incrementally lowered allowing the recoating mechanism (usually a stiff blade or roller) to spread thin, $20\ \mu m$ to $50\ \mu m$, layers of metal powder. While there has been increased industry use in recent years, the inability to ensure repeatable final part properties remains a primary factor preventing the widespread use of AM processes. These properties include tensile and fatigue strength, hardness, surface roughness, and density, all of which are highly dependent on the process parameters and conditions. The localized heating and cooling introduces residual stress that is often location dependent due to changes in geometry or scan strategy [1]. The environmental conditions as well as the part layout have been found to affect the final part properties [2-3]. Additionally, the final mechanical properties of a part depend on the orientation in which a part is built [4].

Though there has been substantial focus on documenting, modeling, and providing solutions for these known sources of variability in the PBF process, focus must also be placed on understanding the role played by the characteristics of the metal powder. Yadroitsev et al., using an analysis of variance, found the particle size distribution (PSD) to be a statistically significant

variable affecting the contact angle of a single track and the ratio of the remelted depth to the height of a single track [5]. Other groups have conducted similar research. Spierings et al. conducted an experiment using three stainless steel powders (316L), each of different size distributions to investigate the effect of the PSD of powder on the density, surface roughness, and mechanical properties of final parts. They found particle size to have significant effect on all three of the dependent variables measured. While it was possible to create 99% dense parts using each powder, the scan strategies needed to be individually optimized for each [6]. In a similar fashion, Gu et al. investigated the microstructural and mechanical properties of AM parts created using a titanium alloy powder (Ti6Al4V) procured from three separate suppliers. Again, using equivalent parameters, powders with different PSDs produced final parts with substantial differences in their tensile properties [7]. A similar comparison is made by Liu et al. using two powder types with similar mean sizes ($< 2\,\mu$m difference), but dissimilar distributions. One of the 316L powders had a log-normal distribution and the other featured a skewing towards smaller particles. Although at low energy densities (created by either reducing the beam size or increasing the scan speed) the log-normally distributed powder created parts with significantly lower density and substantially rougher side surfaces, the same powder also produced parts with higher tensile properties [8].

All of the aforementioned findings share one thing in common: they serve as evidence that the PSD of the powder used in AM plays a significant role in determining the final part properties. Recognizing this, it becomes apparent that any sources of variability in the PSD of AM powders must be identified and documented. Slotwinski et al. have found PSD of the AM materials to vary depending on the location in the machine [9]. They found that particles larger than 60 µm were more likely to be spread past the build plate and consequently were not used in the build. The variability was attributed to the limited space (a layer height of 20 µm was used in the experiment) between the lower edge of the recoating mechanism and the prior layer of powder. It was theorized that the larger particles were unable to easily pass under the recoater, and were therefore spread over the powder bed and eventually into the collector. Besides this work, there has been very little published that characterizes spatial inconsistencies of the PSD of AM powders.

As it has been clearly shown that the PSD affects the repeatability of the PBF process and a variability in the PSD as a function of the location in the machine was documented [9], it is paramount that this spatial dependence of the PSD be investigated further. The work presented here investigates sources of variability in the PSD of metal AM powder in three situations: in a container in an as-received condition, in a loose powder bed, and in a powder bed with solidified parts.

2 Experimental Procedure

2.1 Sampling

While the situation in which powder is collected may differ, the basic tools remain the same. Firstly, the powder must be extracted in a controlled manner. As directed in ASTM B215 [10], a slot sampler should be used to extract powder in a loose, bulk condition. The conventional slot sampler, similar to a soil core sampler, is used to collect a continuous cylindrical volume of powder, making it nearly impossible to keep a free-flowing granular material from mixing during the sampling. In order to quantify any vertical segregation of particle sizes, discrete volumes must be sampled at incrementally deeper positions. The custom slot sampler, shown in Figure 1, features a conical tip to reduce the disturbance of the bulk powder as the device is plunged into the granular material as well as both a rotating collecting shaft that allows a controlled opening or

closing of the sampling volumes and a handle that provides ergonomic handling of the sampler. The volumes of the collection pockets are chosen to provide an optimal sample mass ($\approx$0.3 g) for the later-described particle size analysis. While too little powder will decrease the accuracy of the PSD by measuring less powder, alternately, if too much powder is collected, the powder must be resampled, which often introduces biases depending on the sampling location. These biases can be minimized or possibly completely avoided with the use of a proper sampling technique like a riffler. Riffling is a technique that allows a bulk powder to be divided into smaller samples, each of which is a good representation of the original powder. The technique, suggested in ASTM B215 and illustrated in Figure 2, consists of the collection of powder from a stream of powder. The bulk powder is directed towards a chute by means of vibration. Upon exiting the chute, the powder is allowed to fall into a series of moving containers. If any segregation was present, it will be divided amongst each of the containers, assuming the riffler is operated correctly. With increasing numbers of rotations of the collection containers, the effectiveness of the operation increases, but the rule-of-thumb is that 100 rotations must be completed by the time all of the powder has flown through the chute.

The other situation in which powder must be collected is when it is sparsely spread on a solidified AM part. The part's upper surface is relatively rough (R_a from 9 μm to 19 μm [8]), which makes collection difficult. Mechanical removal, such as brushing or scraping, is ineffective in removing the powder. An apparatus was designed and fabricated allowing a vacuum to be used to collect powder in a controlled manner. This device will be described in detail in a later publication.
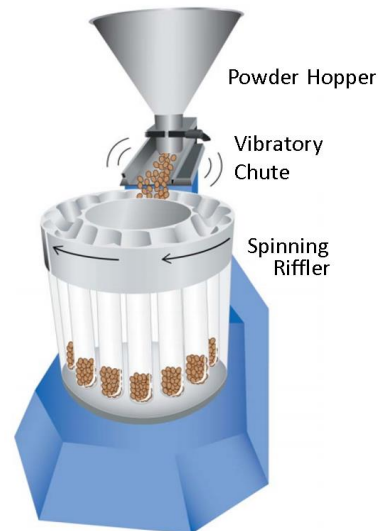

Figure 1: Custom slot sampler

Figure 2: Schematic of a spinning riffler [10]

2.1.1 Powder As-received

Three 10 kg containers of stainless steel powder (17-4PH) are used to investigate any segregation of the powder's PSD. Most powder manufacturers ship metal powders in a plastic container that has been filled with argon prior to being sealed shut. The container often contains a silica gel desiccant to absorb any moisture. Each of the containers is opened and the desiccant

removed prior to being sampled with the slot sampler. All containers are sampled at their radial centers at three different heights. The lowermost sample has its vertical center at a height approximately 7 mm from the bottom, while the middle and top samples are approximately 44 mm and 88.5 mm from the bottom, respectively. Each of the samples taken is approximately three grams, which, being too large for the particle size analyzer, is riffled into eight samples prior to being measured.

2.1.2 Powder Bed

A loose powder bed is created by repeatedly spreading 20 µm layers of powder in a commercial PBF system without scanning the laser. The system uses a dispensing bed that moves incrementally up, providing powder to be spread across the build plate. The bed is built up to 2500 layers (50 mm total depth) prior to being sampled. The custom slot sampler, shown in Figure 1, is used to sample powder at nine locations in the build bed (see Figure 3) and one centrally located position in the dispenser.
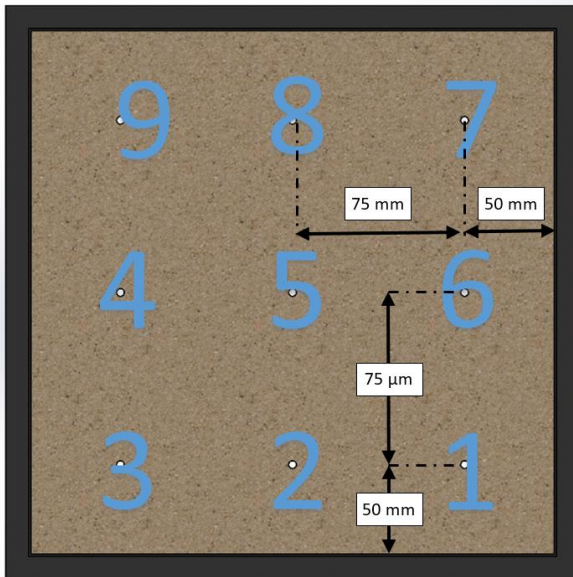

Figure 3: Sequence and locations of powder collection; the dark outlined perimeter refers to the outer edges of the build plate
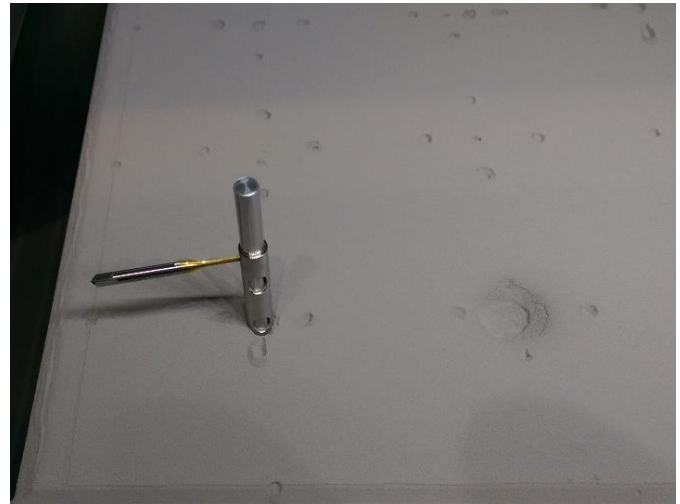

Figure 4: Custom slot sampler extracting powder in position #3

2.1.3 Powder on a Solidified Part

In order to be able to extract powder from the surface of a solidified part, the aforementioned vacuum apparatus is used. Filters with a pore size of less than 6 µm ensure that no particles pass through the filter. Powder is also extracted from before and after the part (where right refers to the side of the machine in which powder is dispensed) in order to allow the effect that the part's presence has on the spreading of powder to be better understood. The custom slot sampler (Figure 4) is used to extract powder from the part's vicinity. The sampler is pushed against the part's right side so that the outer edges of each are tangential. This is done to ensure that the sample extracted was from powder that was deposited onto the loose powder bed immediately prior to the recoater passing over the part. Powder is taken in a similar manner on the Collector

side to ensure the sample taken is from the powder that was pushed over the part and deposited in the region to the part's left (see Figure 5 & 6).
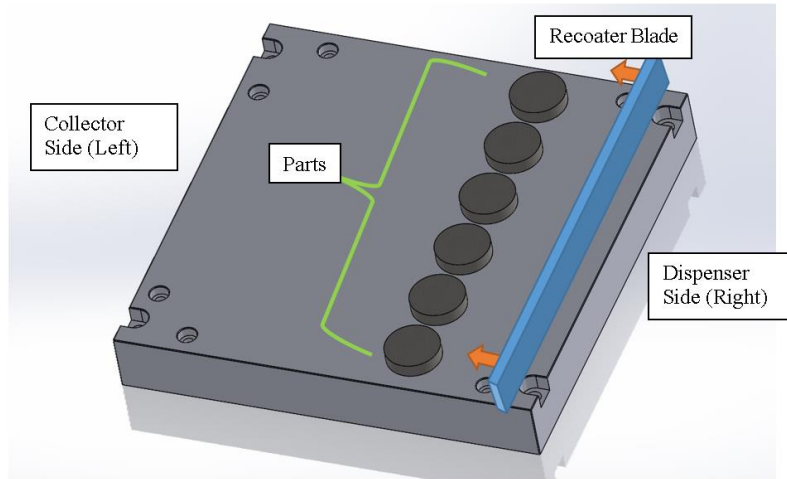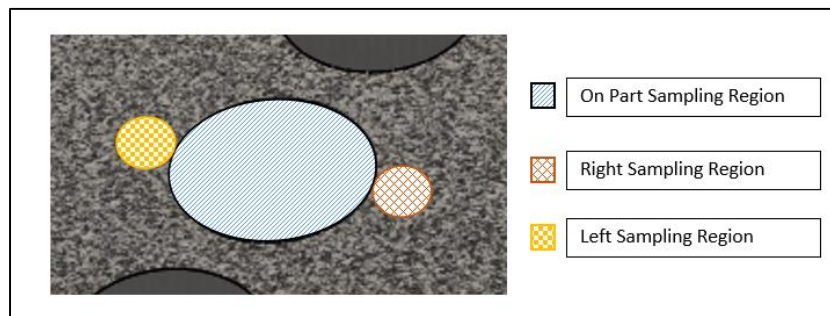

Figure 5: Build plate and part layout

Figure 6: Sampling regions on, right, and left of solidified part

2.2 Measuring Size and PSD

An optically-based particle size analyzer is used to characterize the powder. The device uses two charge-coupled device cameras to conduct a dynamic image analysis method (ISO 13322-2). One of the cameras uses a higher magnification to resolve smaller particles and provide more accurate morphology measurements. The camera has a resolution of about 1 µm per pixel. There are numerous metrics that can be used to characterize the size of a particle, not to mention its morphology [11]. When measuring a particle that is not perfectly spherical, the methods used to characterize even something as simple as the diameter are not direct. Figure 7 illustrates a few of these methods. The Martin diameter uses the area bisector of the particle's profile, while the Feret or caliper diameter is the distance between two tangent lines that are perpendicular to the measurement direction. Another commonly used metric is the projected area diameter, which is the diameter of a circle having an equivalent area as the particle. Since nearly all of the particles in AM metal powders are nearly spherical and convex [9], the Feret or caliper diameter is reported in this paper. Additionally, the results from a size analysis can be reported in terms of the number, weight, or volume of the particles. Since the optically-based method measures the area of the particle's projection, and this area of a nearly spherical particle can easily be converted to volume, the results will be reported in terms of volume.
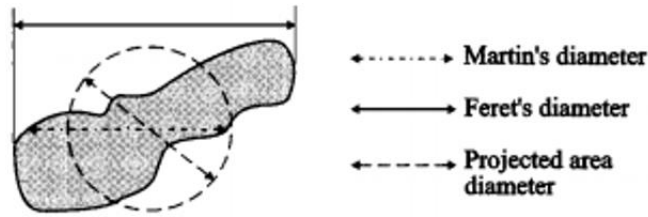
Figure 7: Methods of describing a non-spherical particle's diameter [12]

Results from particle size measurements are most often reported as either a cumulative or a frequency size distribution. A frequency size distribution plot is similar to a histogram with a series of size bins on the *x*-axis and the percentage of their respective populations (based on number, volume, or mass) on the *y*-axis. A cumulative size distribution also has the size of the particle on the *x*-axis, but the *y*-axis is displayed in terms of the accumulative percentage of the particles. As mentioned, the metric of "particle size" can be specified in many ways; this paper will report the particle size in terms of the Feret diameter. The cumulative and frequency distribution will always be reported in terms of particle volume. The D_{10}, D_{50}, and D_{90} of a sample's PSD refer to the maximum size corresponding to 10 %, 50 %, or 90 % of the particles. Unless otherwise noted, each powder sample is measured five times, and the plotted PSDs use the average of these five measurements for each size class with the standard deviation plotted as error bars.

3 Results and Discussion

3.1 Powder As-received

Table 1 and Figures 8-10 illustrate the PSDs at the three heights of the three containers sampled. It should be noted that the containers sampled were known to have dissimilar PSDs. To show this, the frequency distribution of the top location of each powder is plotted in Figure 11. Powder B has virtually no segregation of particle sizes, while Powder A and Powder C seem to have a slight variability with height. The sample taken from the middle height has the smallest particles of all three of the powders, though as shown in Figure 9, the change in the PSD of Powder B's samples is almost indiscernible. From this result, the difference in the initial PSDs seems to affect the segregation seen in the containers. However, the magnitude of the variation is on the same order as the 1 µm resolution of the particle size analyzer, and, considering the ranges of the PSD's standard deviations ($.04 < \sigma < .68$) shown in Table 1, this difference may be negligible.

Table 1: D_{10}, D_{50}, and D_{90} of the maximum Feret diameters and respective locations of powder collected from containers

|	D_{10}		D_{50}		D_{90}	
Powder (location)	Average	σ	Average	σ	Average	σ
Powder A (top)	21.12	0.04	31.34	0.11	47.96	0.30
Powder A (middle)	20.28	0.15	30.04	0.30	45.84	0.50
Powder A (bottom)	20.82	0.22	30.74	0.26	46.80	0.51
Powder B (top)	26.12	0.08	37.86	0.21	55.98	0.68
Powder B (middle)	25.94	0.11	37.68	0.15	55.30	0.41
Powder B (bottom)	26.40	0.07	38.10	0.07	55.78	0.45
Powder C (top)	23.76	0.11	37.40	0.14	56.08	0.19
Powder C (middle)	22.78	0.08	35.46	0.13	54.48	0.26
Powder C (bottom)	23.88	0.08	37.04	0.17	55.58	0.24
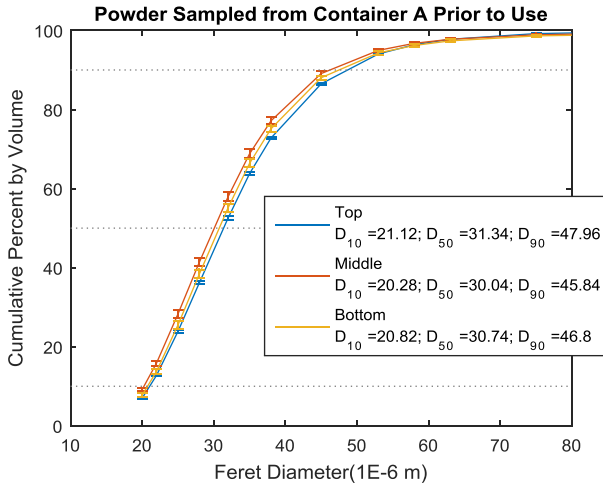
Figure 8: Cumulative size distribution of the maximum Feret diameter of the powder sampled from three heights in the Powder A container
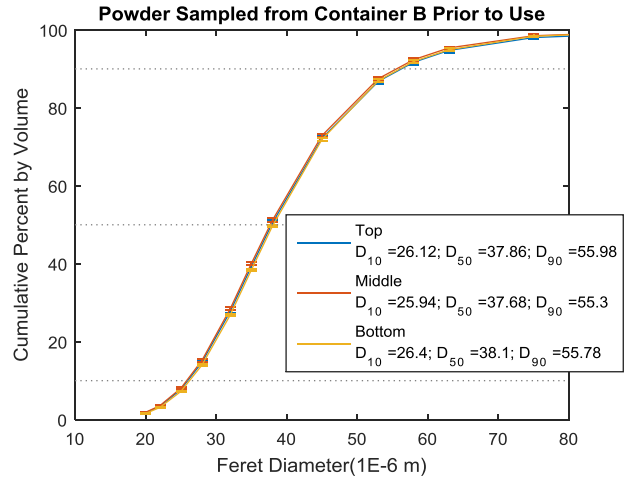

Figure 9: Cumulative size distribution of the maximum Feret diameter of the powder sampled from three heights in the Powder B container
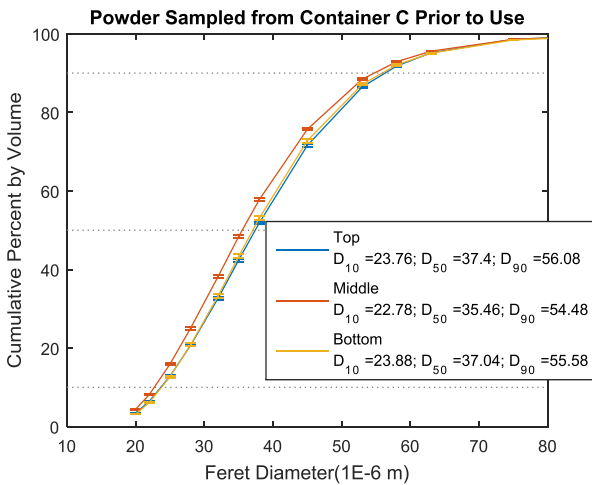

Figure 10: Cumulative size distribution of the maximum Feret diameter of the powder sampled from three heights in the Powder C container
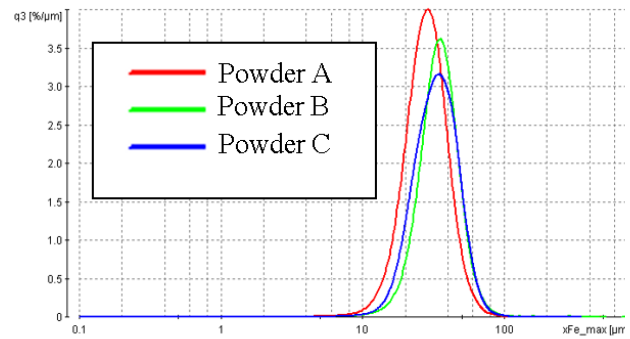

Figure 11: Frequency size distribution of the maximum Feret diameter of the powder sampled from the 'Top' location from each of the powder types

Box and whisker plots of the D_{10} are shown in Figure 12. The blue outline represents the 25th and 75th percentiles of the five measurements taken while the red line shows the median. The 'whiskers' (referring to the black lines) are the range of all values that are not considered outliers. A datum is considered an outlier if it is larger than $q3 + 1.5(q3 - q1)$ or smaller than $q1 - 1.5(q3 - q1)$, where q1 represents the 25th quartile and q3 the 75th. Figure 12, as well as Table 1, show the difference between the three locations. The powder sampled from the 'middle' location is smaller in all three powder types, but the difference is much more prevalent in Powder C and Powder A. A similar trend is seen in the D_{50} and D_{90} values. This vertically centered concentration of smaller

particles may be due to the manner in which the powder was loaded into the container or the disturbance from handling and transportation. Jenike theorized [13], Rémi and Meakin modeled [14], and Savage and Lun showed empirically [15] that finer particles often concentrate near the center of a pile of powder that has been poured. The smaller particles tend to cohere to one another, while the larger particles roll off to the side more easily. It is possible this same mechanism is driving the segregation seen here. As the container is rotated and jostled, the larger particles may move more easily to the extremities of the container. These small variations in the PSD as a function of height likely do not warrant the need for mixing prior to use. It is noted that more research is needed to verify these findings, as this is a narrow view of this segregation.
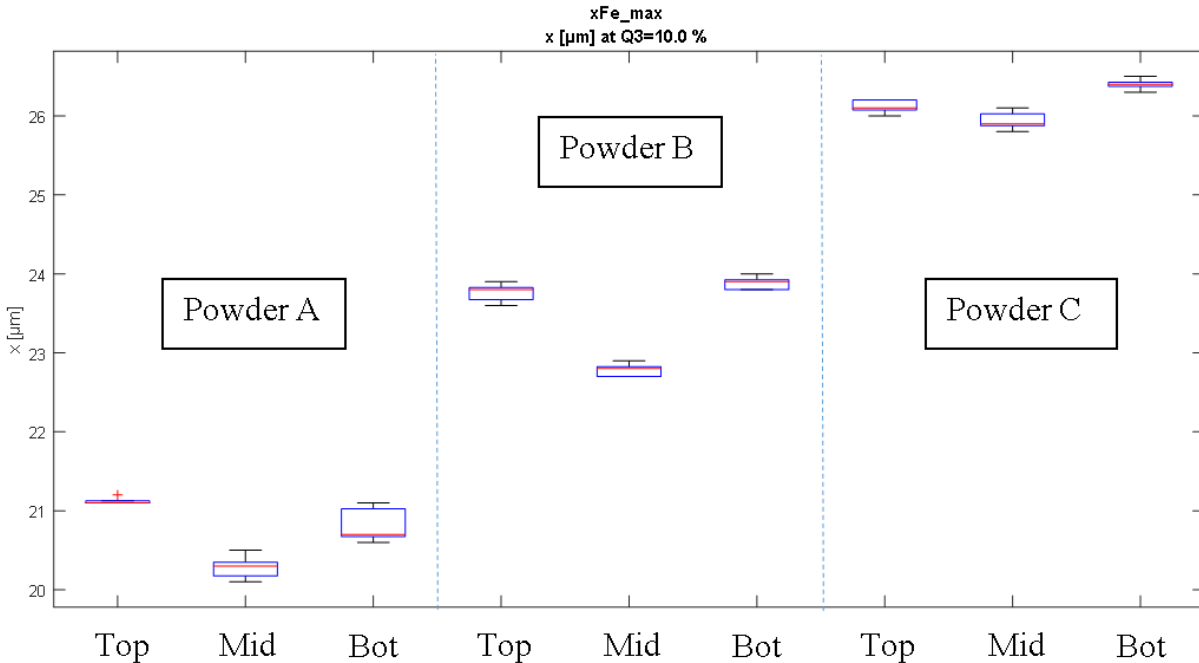

Figure 12: Box plots including 25th and 75th percentiles, median, range and outliers of D_{10} values of maximum Feret diameter; values are volume-based and data points are considered outliers if larger than $q3 + 1.5(q3 − q1)$ or smaller than $q1 − 1.5(q3 − q1)$

3.2 Powder Bed Sampling

Shown in Figure 13, there is very little difference in the powder sampled across the loose powder bed. The D_{50} of the powder sampled shows the largest range of size at 1.5 µm, which is very close to the 1 µm resolution of the optical particle size analyzer. As the variability of the PSDs approach this resolution, concerns regarding the uncertainty introduced throughout the experiment arise. Furthermore, the standard deviation from the five measurements used in calculating the PSDs ranges from 0.09 µm to 0.74 µm (Table 2) which is of a similar magnitude as the ranges documented. These trends are representative of what is seen in other samples.

Powder Sampled from Loose Powder Bed

Legend:
- Position #9: $D_{10} = 22.78$; $D_{50} = 35.88$; $D_{90} = 55$
- Position #8: $D_{10} = 21.84$; $D_{50} = 34.38$; $D_{90} = 54.54$
- Position #7: $D_{10} = 22.4$; $D_{50} = 34.86$; $D_{90} = 53.56$
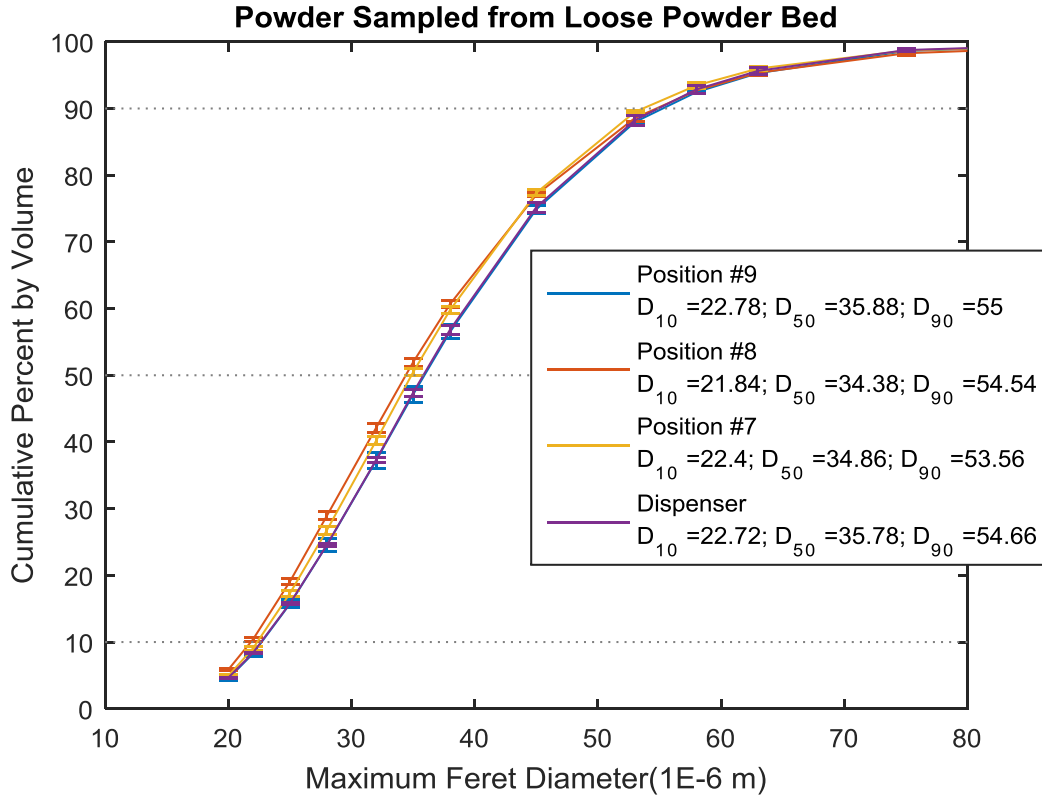- Dispenser: $D_{10} = 22.72$; $D_{50} = 35.78$; $D_{90} = 54.66$

Figure 13: Cumulative size distribution (volume-based maximum Feret diameter) of powder sampled from a loosely spread powder bed using the custom slot sampler

Table 2 lists the standard deviations (σ) and D_{10}, D_{50}, and D_{90} of each of the powder samples from the '7'- '8'- '9' row (see Figure 3 for collection locations). The trends seen here are indicative of a spreading process that has little influence on the trends previously seen in the PSD of powder in the PBF process. This is potentially due to the loose, unpacked nature of the powder bed. While a limited gap between the recoating blade and the part surface or substrate limits the size of particles that can pass under, a loose powder bed may allow larger particles to embed themselves into the previously spread particles. The next section explores the influence of solidified parts on the PSD of the spread powder.

Table 2: D_{10}, D_{50}, D_{90} and standard deviations of the maximum Feret diameters and respective locations (diagram in Figure 3)

Powder Location	D_{10}		D_{50}		D_{90}	
	Average (μm)	σ (μm)	Average (μm)	σ (μm)	Average (μm)	σ (μm)
7	22.40	0.12	34.86	0.17	53.56	0.29
8	21.84	0.09	34.38	0.22	54.54	0.51
9	22.78	0.19	35.88	0.36	55.00	0.19
Dispenser (center)	22.72	0.08	35.78	0.16	54.66	0.74

3.3 On and Off Part Sampling

As seen in the previous two sections, there is minimal segregation of particle sizes in the as-received powder and in a spread powder bed, but there has been documented variability in the PSD of powder in the collector versus powder in the dispenser [9]. Therefore, the presence of solidified part surfaces must play a significant role in the segregation of various particle sizes. Figure 14 contains a cumulative size distribution of the powder sampled from the surface as well as from the right and left of a solidified part. As previously mentioned, the right side refers to the side of the part closer to the dispenser. An obvious skew of the size distribution is seen between the powder taken from the part and samples taken from its vicinity. The 'Part' powder is substantially smaller, while the 'Right' powder is only slightly (a range of D_{50} of 1.16 µm) smaller than the 'Left'. There is also a change in the distribution of the 'Part' powder, which is more easily visualized in a frequency distribution (shown in Figure 15). The distributions of the 'Left' and Right samples are similar with a slight skew towards smaller particles on the Left. The PSD of the Part powder has substantially smaller particles (D_{50} =31.54 µm compared to 35.08 µm and 36.24 µm for the 'Left' and 'Right' samples, respectively) and is narrower. The surface of the solidified part appears to act as a filter of the powder being spread. While the step in the layer height is only 20 µm, due to the densification of the loose powder during the melting and solidification, the actual vertical distance between the recoater blade's underside and the solidified part surface is substantially larger. Using a similar method as theorized in [16], the effective, steady-state layer height for a 20 µm build plate movement is approximately 33 µm, assuming a 99% dense final part. Since this is around the D_{50} (maximum Feret diameter) of the powder spread, a large portion of particles are unable to pass under the recoating blade. Though due to the relatively rough top surface of the solidified part, the actual effective layer thickness is highly variable and might allow larger particles to settle in the valleys between laser tracks.

Powder Sampled from Solidified Part Surface and Close Proximity

Part
D_{10} =21.4; D_{50} =31.54; D_{90} =49.82
Left
D_{10} =22.94; D_{50} =35.08; D_{90} =53.86
Right
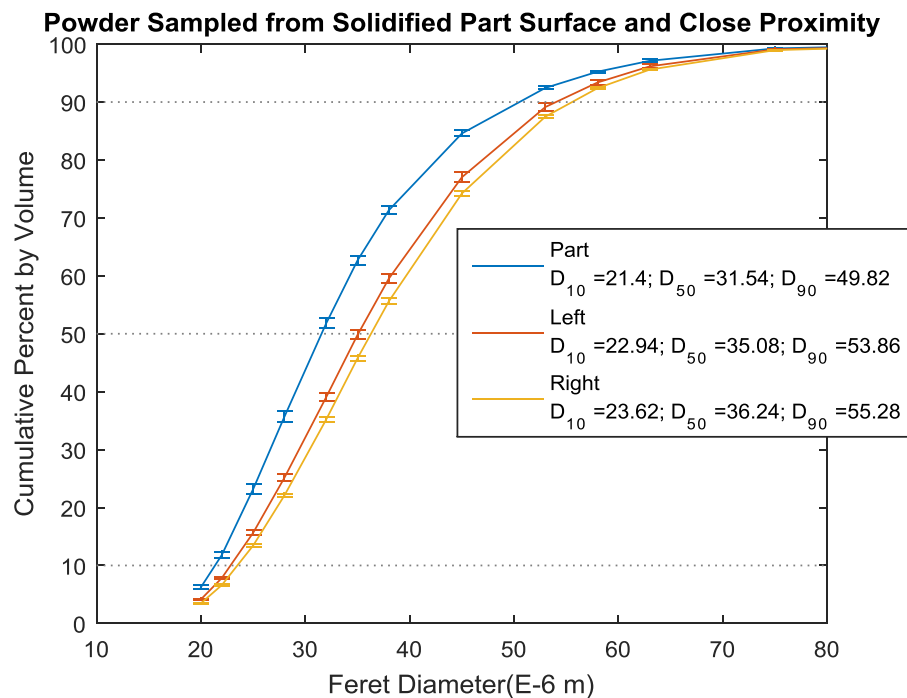D_{10} =23.62; D_{50} =36.24; D_{90} =55.28

Figure 14: Cumulative size distribution (volume-based maximum Feret diameter) of powder sampled from the left, right, and surface of a solidified part
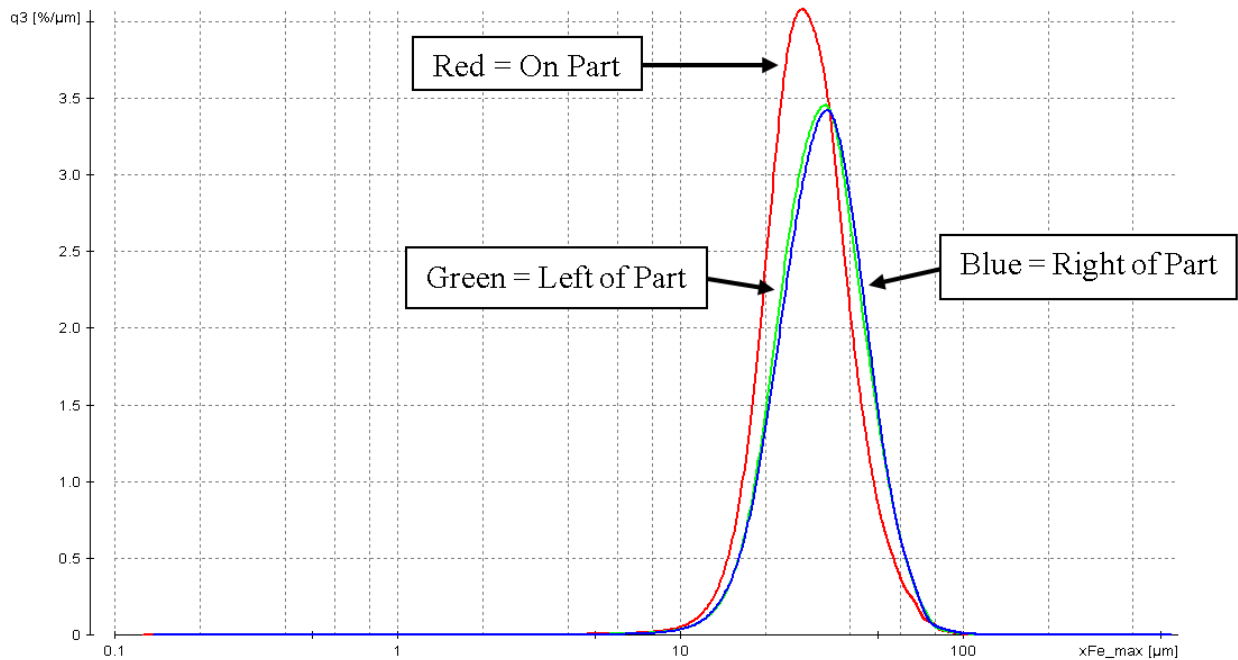
Figure 15: Frequency size distribution of powder sampled from the left, right, and surface of a solidified part; Red = on part, Blue = right of part, Green = left of part

4 Conclusions

The powder spreading in the PBF process is extremely complex. The fact that each powder particle is unique and that the cohesion forces between particles is dependent on the surfaces and geometries of these particles creates a very intricate process. Moreover, the intricate surfaces of solidified parts have been found to influence the spreading. While simplifications can and must be made in modeling efforts (e.g., perfectly spherical particles, smooth surfaces, finite size ranges), empirical analysis of the powder spreading must be conducted to ensure that the correct assumptions are made. The work presented here delineated the segregation of certain particle sizes in three situations. A minimal change in the PSD at different heights of the powder in its as-received condition was seen. There was also very little change in the size of the powder at different locations along the recoating direction of a loose powder bed. Significant differences in the particles collected from the top of a part versus the part's adjacent vicinity was seen, and potential reasons for this have been proposed. It is noted that the work shown here provides only a glimpse into the spatial dependence of the PSD of powder and should not be taken as concrete evidence but rather as a starting point for future research. Further research will focus on closely investigating the interaction between the powder and the recoating mechanism via empirical analysis as well as modeling. The rheological behavior of AM powders will be compared to the performance of the spreading in the PBF process.

References

[1] Mercelis, Peter, and Jean-Pierre Kruth. "Residual stresses in selective laser sintering and selective laser melting." *Rapid Prototyping Journal* 12, no. 5 (2006): 254-265.

[2] Simchi, A. "Direct laser sintering of metal powders: Mechanism, kinetics and microstructural features." *Materials Science and Engineering*: A 428, no. 1 (2006): 148-158.

[3] S. Dadbakhsh, L. Hao, and N. Sewell. "Effect of Selective Laser Melting Layout on the Quality of Stainless Steel Parts." *Rapid Prototyping Journal* 18, no. 3 (April 20, 2012): 241–49. doi:10.1108/13552541211218216.

[4] Paul, Ratnadeep, Sam Anand, and Frank Gerner. "Effect of thermal deformation on part errors in metal powder based additive manufacturing processes." *Journal of Manufacturing Science and Engineering* 136, no. 3 (2014): 031009.

[5] Yadroitsev, Igor, Ina Yadroitsava, Philippe Bertrand, and Igor Smurov. "Factor analysis of selective laser melting process parameters and geometrical characteristics of synthesized single tracks." *Rapid Prototyping Journal* 18, no. 3 (2012): 201-208

[6] Spierings, A.B., N. Herres, and G. Levy. "Influence of the Particle Size Distribution on Surface Quality and Mechanical Properties in Additive Manufactured Stainless Steel Parts." I*n 21st Annual International Solid Freeform Fabrication Symposium - An Additive Manufacturing Conference, SFF* 2010, 397–406. Austin, TX, United states, 2010.

[7] Gu, Hengfeng, Haijun Gong, J. J. S. Dilip, Deepankar Pal, Adam Hicks, Heather Doak, and Brent Stucker. "Effects of powder variation on the microstructure and tensile strength of Ti6Al4V parts fabricated by selective laser melting." *In Proceedings of the 25th Solid Freeform Fabrication Symposium*, Austin, Texas, USA, pp. 470-483. 2014.

[8] Liu, Bochuan, Ricky Wildman, Christopher Tuck, Ian Ashcroft, and Richard Hague. "Investigation the effect of particle size distribution on processing parameters optimisation in selective laser melting process." *In International solid freeform fabrication symposium: an additive manufacturing conference*. University of Texas at Austin, Austin, pp. 227-238. 2011.

[9] Slotwinski, J. A., E. J. Garboczi, P. E. Stutzman, C. F. Ferraris, S. S. Watson, and M. A. Peltz. "Characterization of Metal Powders Used for Additive Manufacturing." *Journal of Research of the National Institute of Standards and Technology* 119 (October 2014): 460. doi:10.6028/jres.119.018.

[10] ASTM Standard B215-15, 2015, "Standard Practices for Sampling Metal Powders." ASTM International, West Conshohocken, PA, 2003, http://dx.doi.org/10.1520/B0215-15.

[11] Cooke, April, and John Slotwinski. "Properties of metal powders for additive manufacturing: a review of the state of the art of metal powder property testing." US Department of Commerce, National Institute of Standards and Technology, 2012.

[12] Fan, Liang-Shih, and Chao Zhu. *Principles of gas-solid flows*. Cambridge University Press, 2005.

[13] Jenike, Andrew W. "Storage and flow of solids, bulletin no. 123." *Bulletin of the University of Utah* 53, no. 26 (1964).

[14] Jullien, Rémi, and Paul Meakin. "A mechanism for particle size segregation in three dimensions." *Nature* 344, no. 6265 (1990): 425-427.

[15] Savage, S. B., and C. K. K. Lun. "Particle size segregation in inclined chute flow of dry cohesionless granular solids." *Journal of Fluid Mechanics* 189 (1988): 311-335.

[16] Spierings, A. B., and G. Levy. "Comparison of density of stainless steel 316L parts produced with selective laser melting using different powder grades." *In Proceedings of the Annual International Solid Freeform Fabrication Symposium*, pp. 342-353. Austin, TX, 2009.